Available online at www.sciencedirect.com
ScienceDirect
Acta Materialia 56 (2008) 1106–1113
Acta MATERIALIA
www.elsevier.com/locate/actamat

The influence of geometry on grain boundary motion and rotation

N. Bernstein *

Naval Research Laboratory, Center for Computational Material Science, NRL Code 6390, 4555 Overlook Ave SW, Washington, DC 20375, USA

Received 7 August 2007; received in revised form 1 November 2007; accepted 2 November 2007
Available online 21 December 2007

Abstract

Recent theoretical and simulation studies indicate that grain boundary motion is coupled to the translation and rotation of the adjacent grains. However, the geometry of the system can strongly modify this coupling. We simulate the evolution of grains in two geometries that are similar to experimental systems that have been studied. The first, a small circular grain embedded in a matrix consisting of two other grains, shows that rotation can be suppressed by geometric frustration, but the coupling slows the grain boundary motion. The second, a bicrystal cut into a wedge shape, shows that free boundaries can act as sinks for grain boundary dislocations thereby stopping or even reversing the rotation caused by grain boundary motion. These results show that an experimentally relevant theory of grain boundary motion needs to consider the effects of microstructure and sample geometry.
Published by Elsevier Ltd on behalf of Acta Materialia Inc.

Keywords: Grain boundary migration; Molecular dynamics

1. Introduction

The properties of polycrystalline materials are often strongly dependent on their microstructure. There is therefore great interest in understanding the nature and evolution of grain boundaries (GBs). Recent atomistic simulations and theoretical analysis suggest that the motion of grain boundaries is inherently coupled to the translation and rotation of the adjacent grains, and can even lead to an increasing misorientation angle as a function of time [1–6]. Attempts to observe this coupling experimentally, recently reviewed in Refs. [5,6], have shown some evidence for it in rectangular bicrystals under shear [7–12], thin single-crystal grains on a surface [13–16] and gold films [17], but other studies of microstructure evolution have not seen grain rotation or translation [18–21].

One reason (noted by Cahn and Taylor [2]) why this coupling appears in the simulations but not in some experiments is that the geometries of the samples are very different. Simulations have primarily studied simple geometries, where the effects of the coupling can be maximized, e.g. a cylindrical grain surrounded by a single surrounding matrix grain, or two rectangular grains with a flat GB. Experiments that did not show coupling, on the other hand, studied complex geometries consisting of irregularly shaped grains in a complicated matrix, or wedge-shaped bicrystals with finite extent along the GB. In this paper, we present atomistic simulations of GB motion in simplified geometries that capture the essential features of some experimental geometries. These comprise a circular grain in a single grain matrix for comparison with earlier work, a circular grain bounded by two different grains and a bicrystal cut into a wedge shape. Although our length and time scales are much shorter than those used in experiments, our observations reveal how the GB network and system geometry can affect GB motion.

2. Methods

We use a molecular dynamics simulation to evolve the systems in time with the fourth-order gear predictor–corrector algorithm [22]. The atoms interact through a model Lennard–Jones potential, with $\sigma = 1$ Å and $\epsilon = 1$ eV. The

* Tel.: +1 202 404 8628; fax: +1 202 404 7546.
E-mail address: noam.bernstein@nrl.navy.mil

1359-6454/$30.00 Published by Elsevier Ltd on behalf of Acta Materialia Inc.
doi:10.1016/j.actamat.2007.11.002

potential is cut off at $r = 1.5$ Å and shifted so that there is no discontinuity in energy. Each atom is assigned a mass of 1 amu, and the time step for propagation is set to 0.01 fs.

The underlying crystal is a two-dimensional triangular lattice, allowing us to form tilt GBs. The GBs are formed by cutting out pieces from appropriately rotated lattices, putting them together and minimizing the energy of the system by relaxing with respect to atomic positions using the conjugate-gradient algorithm [23]. Each system has finite extent and free boundary conditions. The system is then simulated at constant energy with kinetic energy equivalent to a temperature of about 300 K. Note that, since the potential represents a model system rather than any particular material, the energy (and therefore temperature), length and time scales are essentially arbitrary, and not directly comparable to any experiment.

To analyze the simulation results, it is helpful to be able to automatically assign the atoms in the simulated system to each grain. We do this by computing a nearest neighbor list for each atom, and then computing an angular structure factor, i.e.

$$S_n(k) = \sum_l \exp\left(ik \arctan\left(\frac{r^y_{nl}}{r^x_{nl}}\right)\right) \quad (1)$$

where r^α_{nl} is the Cartesian α component of the relative position of atoms n and l. Since each atom has six neighbors in the triangular lattice, $S_n(6)$ probes the rotation of the local neighborhood of atom n. The phase of S indicates which grain the atom belongs to. This approach works well as long as the misorientation angle is not too small; in the one case where the misorientation is close to 5°, once one of the grains becomes sufficiently small it can no longer be reliably distinguished from its neighbor.

The positions of triple-junctions (TJs) are tracked manually in the visualized images where atoms are colored by their automatic grain assignment. The position values plotted and tabulated below are defined as the distance from an atom adjacent to the TJ to the nearest atom on the free surface of the cylindrical simulated system. The discreteness of the lattice causes an inherent uncertainly of about 2σ in this measurement.

3. Results

3.1. Circular grain in single-crystal matrix

To confirm that we see the qualitative behavior seen in previous work, we simulate a single circular grain with diameter of 50 σ in a single grain matrix, forming a low symmetry tilt GB with a misorientation of 10°. The size of the grain and the relative angle of the grain and the matrix are plotted in Fig. 1. Our observation that the grain misorientation increases as it shrinks are consistent with previously published results [1,5]. Visualization of the atomic positions as the system evolves in time is shown Fig. 2. The number of dislocations in the GB decreases

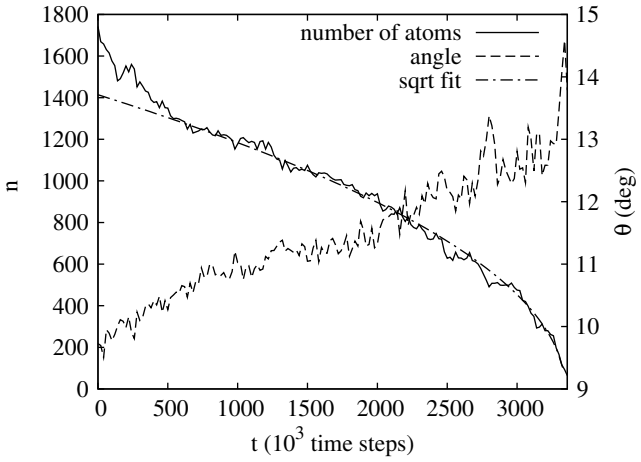

Fig. 1. Number of atoms (with fits to $c(1 - at)^b$ for $b = 0.44$ and $b = 0.56$) and relative angle for a circular grain in a monocrystalline matrix as a function of time.

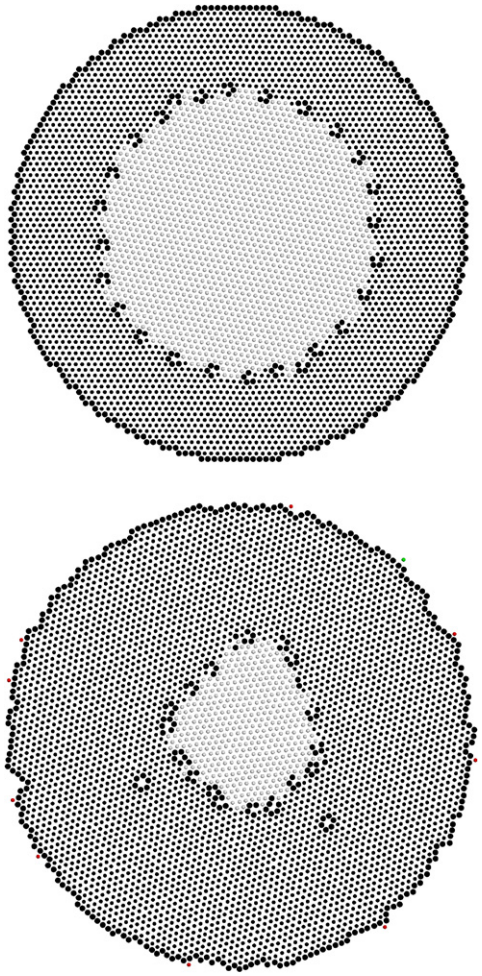

Fig. 2. Visualization of circular grain surrounded by a single matrix grain at $t = 0$ time steps (top) and $t = 3.0 \times 10^6$ time steps (bottom). Colors indicate which grain each atom is assigned to, and larger spheres indicate atoms with coordination other than 6 (cluster of such atoms surround vacancies and dislocation cores).

from 26 at the initial time to 17 at 3.0×10^6 time steps, a factor of 0.65. Since the number of atoms in the grain decreases from 1788 to 488 over the same time, the corresponding change in the GB length is a factor of 0.52, and so the dislocation density increases by a factor of 1.25. This is nearly equal to the ratio of the angles, from 10° to 12.5°. This analysis confirms the basic idea that the rotation is caused by the number of dislocations in the GB decreasing more slowly than the length of the GB [24,1], although the assumption that the number of dislocations is constant is not confirmed. We did not observe any dislocations escaping from the boundary to the free surface, but we did see some dislocation recombination events, as shown in Fig. 3. In this example two dislocations with Burgers vectors $\vec{a}_2$ and $\vec{a}_1 - \vec{a}_2$ combine into a single dislocation with a Burgers vector of $\vec{a}_1$, leaving behind a vacancy. The visualization in Fig. 1 also shows that the GB facets. Such faceting has also be seen in previous simulations [5,25], although at least in some cases, e.g. Fig. 1f in Ref. [5], the faceting was less pronounced and not explicitly discussed. However, the tendency of GBs to facet is certainly well known experimentally [26], and has even been seen to occur during GB motion [27].

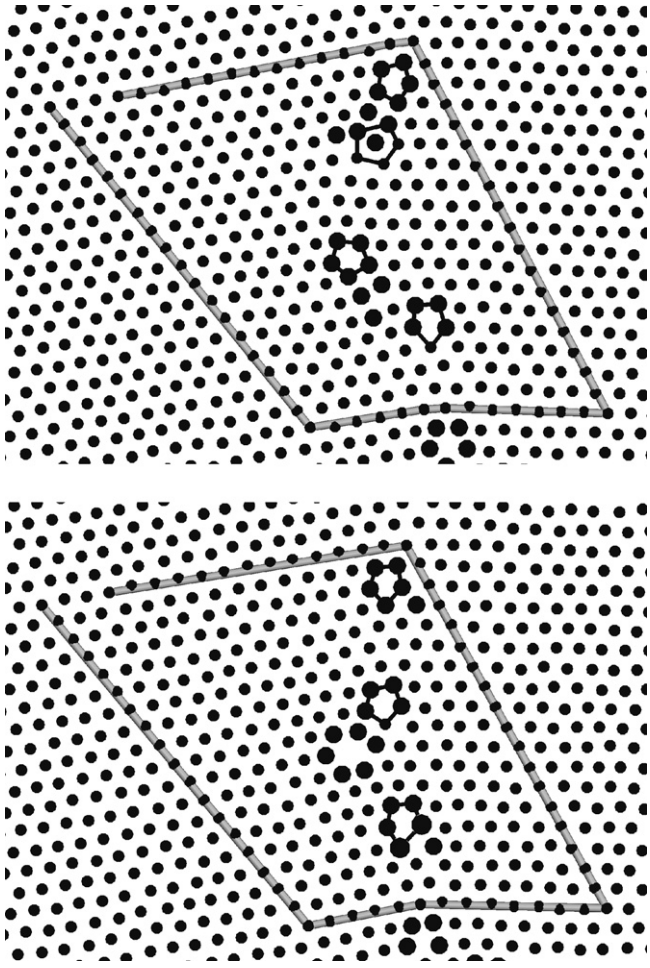

Fig. 3. Atomic configurations at $t = 1.32 \times 10^6$ (top) and 1.34×10^6 time steps (bottom), showing the annihilation of a dislocation. Atom colors and sizes are as in Fig. 2. The gray line shows a Burgers circuit around the group of dislocations, and thin black lines are drawn around each dislocation core.

For this geometry, the rate of motion of the GB can be extracted from the plot of grain area vs. time in Fig. 1. Rath et al. found a power law dependence for the GB speed v as a function of grain radius r of $v = -C/r^m$, where m is an exponent found to be between about 3.5 [20] and 10 [18] for various experimental preparations. This relation for $v(r)$ leads to a grain area A that depends on time as

$$A = c(1 - at)^b \tag{2}$$

where a and c are constants, and b is related to the exponent of the inverse grain radius m via $b = 2/(m+1)$. Excluding an initial transient period, the circular grain's area as a function of time can be fitted by Eq. (2), with a best-fit exponent of $b = 0.56$, i.e. $m = 2.6$. However, the fit is quite insensitive to the exponent over some range, so the fit is nearly as good with $b = 0.44$, i.e. $m = 3.5$, which is quite close to the experimental observations [20]. This result conflicts with Cahn and Taylor's prediction of a linear reduction of grain area with time [2] for small angle tilt boundaries, perhaps because they assume that no dislocations are annihilated during the GB motion.

3.2. Circular grain surrounded by two other grains

A more experimentally relevant geometry than a circular grain in a single-crystal matrix is a small grain bounded by more than one matrix grain. In this case, the different misorientations between the shrinking grain and its neighbors could attempt to drive rotation at different rates or even different directions. To simulate such a situation, we create several bicrystals and embed in each GB a circular grain of diameter 50σ. The geometries, comprising one symmetric and three asymmetric configurations, are summarized in Table 1.

In the symmetric geometry (system 1 in Table 1), the rotation of the circular grain, plotted in Fig. 4, is negligible. The boundaries between the grain and each of its neighbors favor equal and opposite rotation, so overall the rotation is

Table 1
Geometries and GB evolution of a circular grain surrounded by two other grains

System	θ_{12} (°)	θ_1 (°)	θ_2 (°)	$\dot{n}$	Rotation	v_{TJ}
1	20.0	10.0	−10.0	2×10^{-4}	*n*	4×10^{-6}
2	20.0	5.0	−15.0	1×10^{-4}	*n*	0
3	76.4	36.2	−40.2	2×10^{-4}	*y*	3×10^{-6}
4	86.0	40.0	−46.0	3×10^{-4}	*n*	2×10^{-6}

Angle θ_{12} indicates misorientation between two matrix grains, angles θ_1 and θ_2 indicate misorientations between embedded grain and the two surrounding grains, $\dot{n}$ indicates shrinkage rate of grain (in atoms/time step), rot indicates whether the grain rotates during GB motion, and v_{TJ} indicates average triple-junction speed (in σ/time step) (average of two triple-junctions in each system, except system 1 which excludes the triple-junction that is pinned by a void).

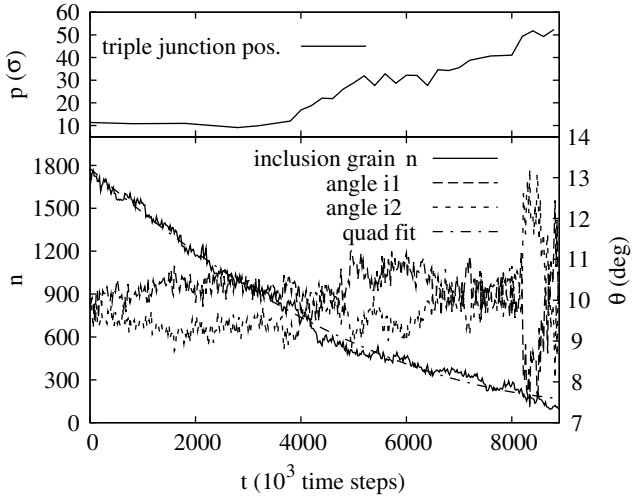

Fig. 4. Bottom panel: number of atoms (with fit to $a + b(t - t0)^2$) and relative angle for a circular grain bounded by two matrix grains with angles of ±10°. Top panel: distance of triple-junction from edge of system (increasing value indicates motion toward the center of the circular grain).

frustrated. Whereas for the single-crystal matrix the dislocations were essentially trapped in the boundary of the grain, forcing an increase in misorientation as the grain shrunk and the dislocations density increased, here the dislocations can move into the newly formed GB between the two matrix grains. The pictures in Fig. 5 show that the GB appears to be pinned on the right. Since there is nothing particular favoring that direction, this is presumably a fluctuation caused by the small system size. There is a void at the pinned triple-junction (TJ), probably caused by a coalescence of dislocations through the mechanism seen in the single-crystal matrix simulation, which we conjecture is causing the pinning. The other TJ, whose distance from the system edge is also plotted in Fig. 4, is initially nearly stationary. As the grain shrinks, the angle subtended by the boundaries between the circular grain and the two matrix grains decreases (from an initial value of 180°), and the effective line tension from these boundaries is able to pull the TJ in toward the center of the circular grain. The average speed of the TJ is listed in Table 1.

While the coupling to the rotation is frustrated, it does have an effect on the rate of GB motion: the grain in the single-crystal matrix took about 1.5×10^6 time steps to shrink from 1750 to 1000 atoms, while the grain in the bicrystal took about 2.5×10^6 time steps. This reduction in GB speed may be thought of as a consequence of a reduction in the driving force, which is the derivative of the free energy of the system as a function of grain size. In the single-crystal matrix case, the driving force comes from the variation of the GB length and the variation in GB energy per unit length, which depends on the misorientation. For a non-rotating circular grain bounded by two symmetric grains, there will be no variation in GB energy per unit length, but there will be an energy cost to create additional GB between the two matrix grains. Because of the complicated dependence of the GB energies on the misorientation angle and the alignment between the GB line and the underlying lattice, it is not feasible to compute these terms explicitly for this geometry.

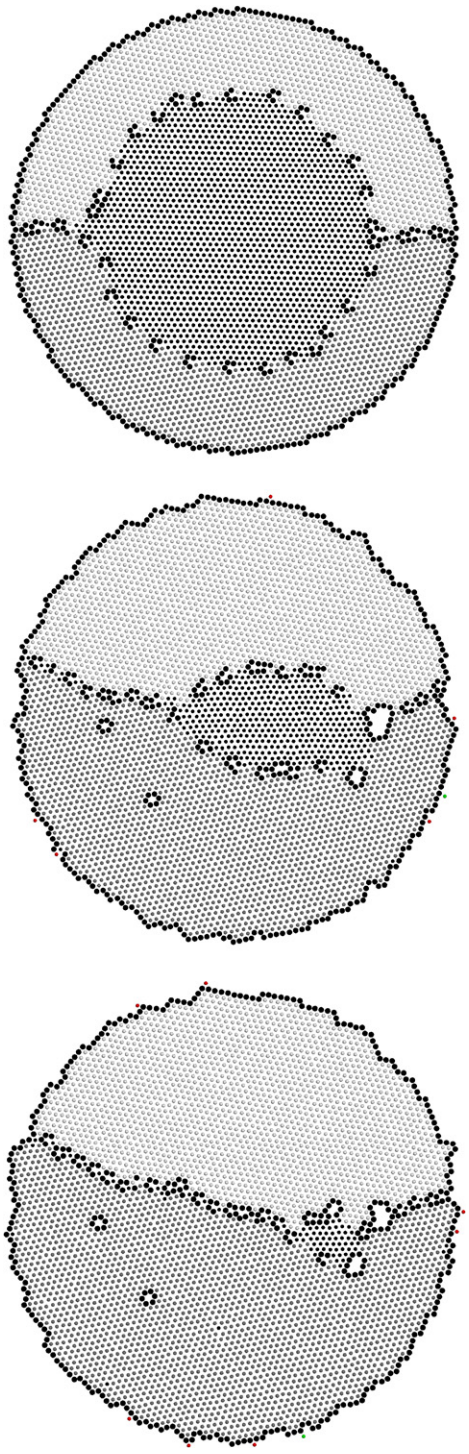

Fig. 5. Visualization of circular grain bounded by two matrix grains at $t = 0$ time steps (top), $t = 5.6 \times 10^6$ time steps (middle) and $t = 9.0 \times 10^6$ time steps (bottom). Color and size of atoms are as in Fig. 2.

The grain area as a function of time is well fitted by a quadratic function, in contradiction with Cahn and Taylor's prediction [2]. However, the geometry of the simulated system is significantly different from the analytical result.

The shrinking grain does not remain circular, and at certain points the inclusion–matrix GBs are pinned at the slowly moving triple-junction formed with the matrix–matrix GB. This leads to a reduction in curvature of the moving GB at large times, and a corresponding reduction in driving force to GB motion. We also cannot exclude the possibility that the area as a function of time is actually linear, with two different slopes at early and late stages of the evolution.

For the symmetric geometry, the directions and magnitude of rotational driving forces cancel out trivially, but this may not be the case for an asymmetric geometry. The evolution of the grain size and rotation angle in a system with a 20.0° GB between the two matrix grains but with an asymmetric embedded grain forming 5.0° and −15.0° GBs (system 2 in Table 1) is plotted in Fig. 6. While grain growth is less steady in this case, it is clear from the plot that there is negligible rotation of the embedded grain with respect to the two matrix grains until the grain is quite small and fluctuations become significant. This observation is consistent with Upmanyu's analysis of GB energy vs. misorientation angle, which shows a roughly constant slope near each energy cusp, so small deviations from symmetry still lead to nearly equal and opposite driving forces for rotation. It is unclear whether the fluctuations in GB motion are simply noise, or evidence of transitions between different quasi-steady-states. Distinguishing these two possibilities would require repeating the simulation many times to obtain a statistical sample, and is beyond the scope of this work. In this system neither TJ is pinned, and both move slightly during the simulation. Initially both move away from the center of the circular grain, as the matrix–matrix GB line tension is able to cause the grain to elongate. Only near the end of the simulation, roughly coincident with the abrupt drop in grain size at about 8.5×10^6 time steps, do the TJs begin to move inward. The overall average of the speed is about 0, although perhaps if the evolution of the system could be followed further the TJs would continue moving inward and show a larger average speed.

Somewhat different behavior is also seen for GBs near the $\Sigma = 19$, $\theta = 38.2°$ cusp identified by Upmanyu et al. [5]. One example is system 3 in Table 1, which forms 36.2° and −40.2° GBs with the matrix grains, whose evolution is plotted in Fig. 7. There are long periods with no grain rotation, punctuated by a relatively abrupt rotation toward the low energy 38.2° misorientation, suggesting that the system shows noise-driven transitions between quasi-steady-states. Since the embedded grain can rotate so that both GBs are transformed into lower energy GBs, it does so, but not in the steady manner that was previously observed for a grain in a single-crystal matrix [5]. Surprisingly, there is no sign of corresponding jumps in the plot of grain size. If both GBs are on the same side of the cusp, for example system 4 in Table 1 with 40° and −46° misorientations, rotation increases the energy of one while decreasing the energy of the other. Since the energy as a function of misorientation near the cusp is roughly linear, there is no net driving force and the grain does not rotate, as shown in Fig. 8. These two systems also show a similar pattern of TJ motion to the symmetrically embedded circular grain, initially stationary and only later moving toward the center of the embedded grain.

The variation of GB motion over time in the asymmetrical inclusion systems depends on the details of the system. The two large misorientation GBs (systems 3 and 4) show a linear variation of area as a function of time, as shown in Figs. 7 and 8, consistent with Cahn and Taylor's calculation [2]. In this case there is very little grain rotation, so the assumption of constant GB energy is probably satisfied (at least approximately) in the simulation, and the

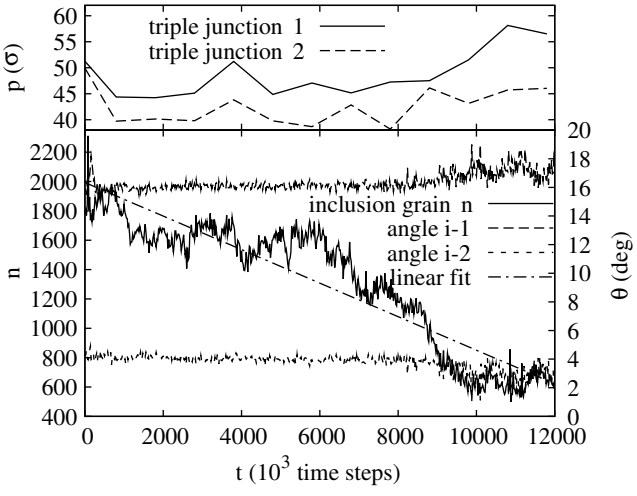

Fig. 6. Bottom panel: number of atoms (with linear fit) and relative angle for a circular grain bounded by two matrix grains with angles of 5° and −15°. Top panel: distance of triple junction from edge of system (increasing value indicates motion toward the center of the circular grain).

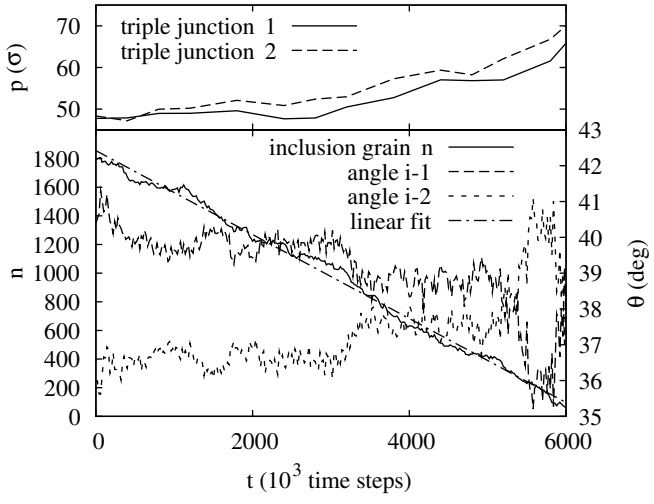

Fig. 7. Bottom panel: number of atoms (with linear fit) and relative angle for a circular grain bounded by two matrix grains with angles of 36.2° and −40.2°. Top panel: distance of triple-junction from edge of system (increasing value indicates motion toward the center of the circular grain).

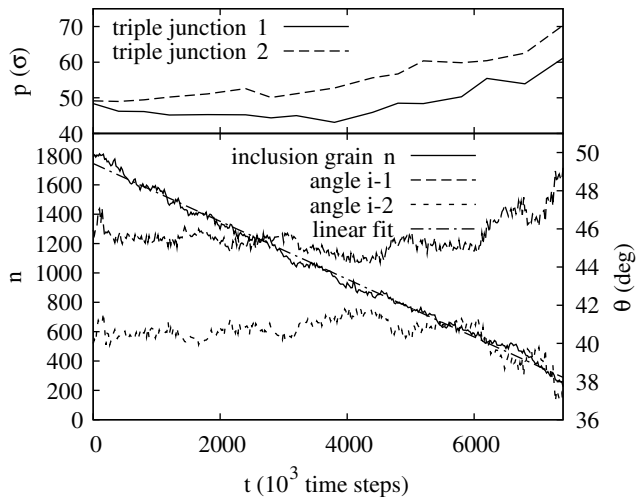

Fig. 8. Bottom panel: number of atoms (and linear fit) and relative angle for a circular grain bounded by two matrix grains with angles of 40.0° and −46.0°. Top panel: distance of triple-junction from edge of system (increasing value indicates motion toward the center of the circular grain).

variation in driving force comes only from the increase in curvature as the grain shrinks. The asymmetric low angle GB (system 2), however, moves in a very unsteady manner. The linear fit, shown in Fig. 6, is roughly consistent with the overall trend, but the deviations are very large. The dependence of the area on time is not well represented by any polynomial function. There is also no corresponding noise in the misorientation angle.

The speed at which the TJs move varies significantly from system to system (Table 1). One of the TJs in the symmetric embedded grain is pinned by a substantial void. The others are all mobile, but there is no obvious correlation between the TJ speed and any other aspect of the GB evolution, including symmetry, GB speed and GB rotation. The only distinctive feature is that the grain which shrinks most unsteadily, system 2 in Table 1, plotted in Fig. 6, shows nearly no net TJ motion at all. In all cases the TJ is initially stationary or moves slightly outward, away from the center of the circular grain. As the grain shrinks the angle subtended by the GBs between the circular grain and the two matrix grains decreases from its initial value of 180°, and the effective line tension pulls the TJ toward the center of the shrinking grain. In system 2 the initial outward motion is relatively large, and the later inward motion relatively small.

3.3. Wedge-shaped sample

The final geometry we study simulates a wedge bicrystal experiment [20]. In this system, a wedge shape is cut from a bicrystal, so that a single well-defined GB is approximately normal to the radial direction of the wedge. There is therefore a driving force for the boundary motion caused by the reduction in area as the GB moves toward the point of the wedge. We create a 10° tilt grain boundary between a circular grain of diameter 100 σ and a single-crystal matrix, and cut out a 60° wedge with its point at the center of the grain. The time evolution of this system in shown in Fig. 9. We use a larger radius grain here as compared to the two previous systems. Simulations of a wedge with a significantly smaller inner grain showed an almost instantaneous coalescence of the two grains through qualitatively different mechanisms involving interactions of the very small number of GB dislocations present and the free surfaces.

As Fig. 10 shows, the evolution of the misorientation in the wedge bicrystal is more complex than our previous examples. The misorientation angle initially increases, but then decreases, increases again, remains approximately constant for a while and finally increases. The increasing misorientation regime occurs via the same mechanism as

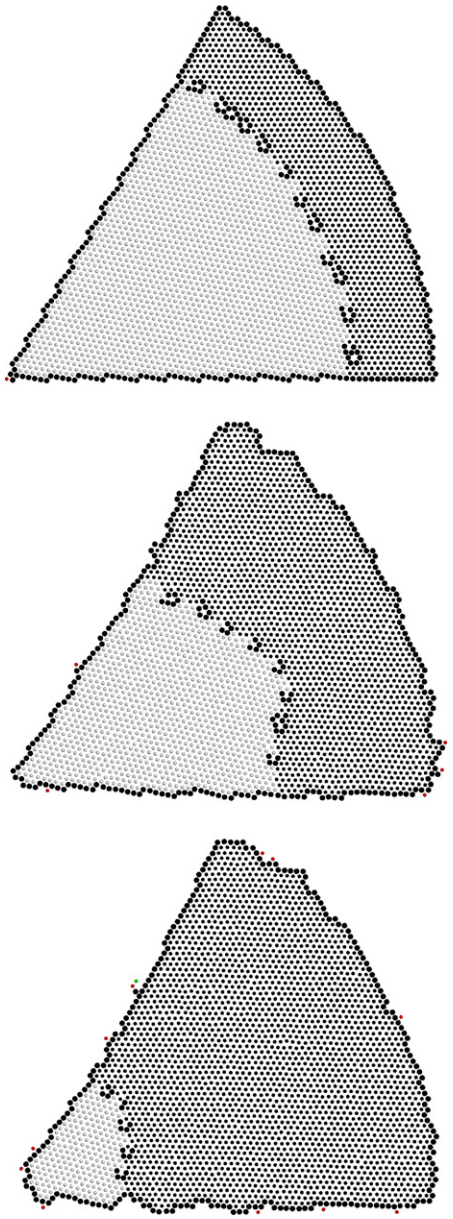

Fig. 9. Visualization of a bicrystal wedge sample at $t = 0$ time steps (top), $t = 21 \times 10^6$ time steps (middle), and $t = 47 \times 10^6$ time steps (bottom). Color and size of atoms are as in Fig. 2.

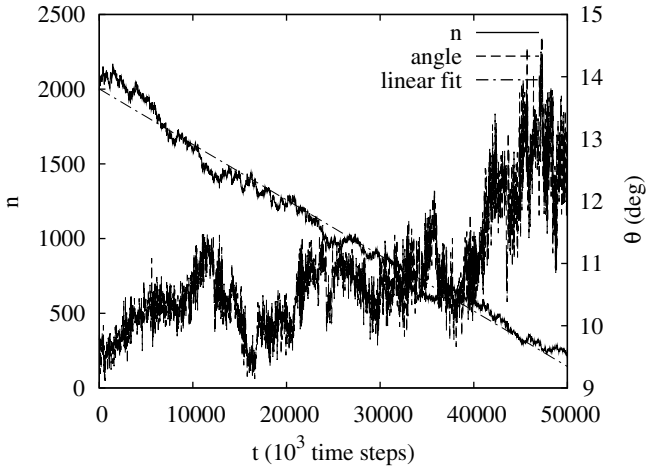

Fig. 10. Number of atoms (and fits to line and to $c(1-at)^b$) and relative orientation for a wedge-shaped bicrystal.

for the grain in a single-crystal matrix, where every GB dislocation moves radially toward the center, and the dislocation density increases with time. The constant misorientation regime can occur if dislocations move, on average, along parallel (not radial) lines approximately normal to the GB. This process would leave the dislocation density constant, and as the GB becomes shorter dislocations will annihilate at the free surfaces. Decreasing misorientation may occur when dislocation positions fluctuate enough to annihilate at the free surfaces. The observed behavior is consistent with simple noise caused by the statistics of the small number of dislocations. Many repetitions of the simulation, which are beyond the scope of this work, would be needed to rule out the possibility of transitions between different steady-states. The negligible amount of rotation through most of the simulation is consistent with the density of dislocations remaining approximately constant as the GB moves, as shown in Fig. 9. The faceting of the GB for this system is particularly pronounced, even more so than for the circular grain in a single-crystal matrix discussed above.

While the geometry of this simulated system is directly analogous to the experimental setup, the length scale is many orders of magnitude smaller [20]. The unsteady evolution of the relative angle is a reflection of the small system size. The number of dislocations in the whole GB is small, and fluctuations caused by the diffusion of the dislocations to the free surfaces are correspondingly large. It is expected that on experimental length scales these fluctuations would be much smaller. Further, in the experiments there is no reason for the dislocations to move radially (leading to grain rotation) except as a fluctuation, since the system can lower its energy even more by moving the GB toward the narrower part of the wedge and simultaneously annihilating dislocations that are near the free surface, leading to no net rotation.

The variation of the area of the grain with time, plotted in Fig. 10, is essentially linear, although it can also be fit by Eq. (2), with $b = 1.38$, i.e. $m = 0.45$. This behavior is quite different from the observations of Rath et al. on similar geometries [20]. It is, however, consistent with the classical expression derived by Cahn and Taylor in the case of no coupling [2]. The wedge geometry allows us to create a sample which is equivalent to the circular grain, but where the character of the GB does not systematically change during GB motion. The simple assumptions of a constant mobility, constant GB energy and driving force that is proportional to curvature (and inversely proportional to grain radius) are indeed applicable to this geometry. The discrepancy with Rath's results suggests that some aspect of the simulation, probably the length and time scales, may limit its applicability to macroscopic scales.

4. Conclusion

The coupling between GB motion and relative translation of the adjacent grains is strongly affected by the geometry of the GB network. While a geometry where there are no constraints on the motion of the grains leads to grain rotation or translation, in other geometries this effect may be suppressed. For example, we have shown here that a symmetric system with a circular grain surrounded by two other grains that produce opposite driving forces for rotation will shrink without rotating. Breaking the symmetry does not necessarily lead to net rotation, unless the particular GBs both favor rotation in the same direction. Even in the latter case, the interaction between the embedded grain and the GB between the two matrix particles leads to much more unsteady and complex GB motion as compared to the single-crystal matrix. The coupling between the GB motion and the rotation can still manifest itself by reducing the GB speed as compared to an equal sized circular grain that is free to rotate with respect to the surrounding single-crystal matrix. The presence of free surfaces, for example in the case of a bicrystal GB undergoing motion driven by the wedge shape of the sample, can also effectively eliminate the coupling by providing a sink for GB dislocations. The speed of GB can also be affected by the geometry. Geometries that lead to minimal grain rotation lead to a linear dependence of grain area as a function of time, in agreement with analytical results that assume a constant GB energy during the motion. However, other geometries can show accelerating GB motion, decelerating motion or even unsteady motion that is not a smooth function of time. Triple-junctions, which were present in our simulations at the points where a circular grain met the boundary between two matrix grains, move at system dependent speeds, although no obvious correlation between the triple-junction speed and other aspects of GB motion were apparent. Geometrical frustration and free surface effects are likely to dominate GB motion in experimentally and technologically relevant microstructures, and need to be taken into account in any comprehensive theory of GB motion.

Acknowledgements

The author would like to thank B.B. Rath and C.S. Pande for helpful discussion of the problem and comments on the manuscript. This work was supported by the Office of Naval Research and the Naval Research Laboratory.

References

[1] Srinivasan SG, Cahn JW. In: Ankem S, Pande C. S, Ovid'ko I, Ranganathan S (Eds.) Science and technology of interfaces. Seattle, WA: TMS; 2002.
[2] Cahn JW, Taylor JE. Acta Mater 2004;52:4887–98.
[3] Suzuki A, Mishin Y. Mater Sci Forum 2005;502:157–62.
[4] Cahn JW, Mishin Y, Suzuki A. Phill Mag 2006;86:3965–80.
[5] Upmanyu M, Srolovitz DJ, Lobkovsky AE, Warren JA, Carter WC. Acta Mater 2006;54:1707–19.
[6] Cahn JW, Mishin Y, Suzuki A. Acta Mater 2006;54:4953–75.
[7] Li CH, Edwards EH, Washburn J, Parker ER. Acta Metall 1953;1:223–9.
[8] Bainbridge DW, Li CH, Edwards EH. Acta Metall 1954;2:322–33.
[9] Fukutomi H, Iseki T, Endo T, Kamijo T. Acta Metall Mater 1991;39:1445–8.
[10] Winning M, Gottstein G, Shvindlerman LS. Acta Mater 2001;49:211–9.
[11] Winning M, Gottstein G, Shvindlerman LS. Acta Mater 2002;50:353–63.
[12] Winning M, Rollett AD. Acta Mater 2005;53:2901–7.
[13] Herrmann G, Gleiter H, Baro G. Acta Metall 1976;24:353–9.
[14] Erb U, Gleiter H. Scripta Metall 1979;13:61–4.
[15] Chan SW, Balluffi RW. Acta Metall 1985;33:1113–9.
[16] Chan SW, Balluffi RW. Acta Metall 1986;34:2191–9.
[17] Harris KE, Singh VV, King AH. Acta Mater 1998;46:2623–33.
[18] Rath BB, Hu H. Trans Met Soc AIME 1969;245:1243–52.
[19] Hu H, Rath BB. Metall Trans 1970;1:3181–4.
[20] Rath BB, Hu H. In: Hu H (Ed.) Nature and behavior of grain boundaries. Seattle, WA: TMS; 1972. 405–35.
[21] B.B. Rath, private communication.
[22] Allen MP, Tildesley DJ. Computer simulations of liquids. Oxford: Oxford University Press; 1987.
[23] Press WH, Teukolsky SA, Vetterling WT, Flannery BP. Numerical recipes in C. Cambridge: Cambridge University Press; 1992.
[24] Li JCM. Trans Met Soc AIME 1969;245:1591–3.
[25] Weingarten NS, Selinger RLB. J Mech Phys Solid 2007;55:1182–95.
[26] Hsieh TE, Balluffi RW. Acta Metall 1989;37:2133–9.
[27] Kirch DM, Zhao B, Molodov DA, Gottstein G. Scripta Mater 2007;56:939–42.